

*cy. 2*

University of California  
Ernest O. Lawrence  
Radiation Laboratory

DIFFUSION OF IRON AND NICKEL IN  
MAGNESIUM OXIDE SINGLE CRYSTALS

Stuart L. Blank and Joseph A. Pask

May 1968

TWO-WEEK LOAN COPY

This is a Library Circulating Copy  
which may be borrowed for two weeks.  
For a personal retention copy, call  
Tech. Info. Division, Ext. 5545

RECEIVED  
LAWRENCE  
RADIATION LABORATORY  
JUL 1 1968  
LIBRARY AND  
DOCUMENTS SECTION

UCRL-17411 Rev.  
*cy. 2*

## **DISCLAIMER**

This document was prepared as an account of work sponsored by the United States Government. While this document is believed to contain correct information, neither the United States Government nor any agency thereof, nor the Regents of the University of California, nor any of their employees, makes any warranty, express or implied, or assumes any legal responsibility for the accuracy, completeness, or usefulness of any information, apparatus, product, or process disclosed, or represents that its use would not infringe privately owned rights. Reference herein to any specific commercial product, process, or service by its trade name, trademark, manufacturer, or otherwise, does not necessarily constitute or imply its endorsement, recommendation, or favoring by the United States Government or any agency thereof, or the Regents of the University of California. The views and opinions of authors expressed herein do not necessarily state or reflect those of the United States Government or any agency thereof or the Regents of the University of California.

Submitted to J. Am. Ceram. Soc.

UNIVERSITY OF CALIFORNIA

Lawrence Radiation Laboratory  
Berkeley, California

AEC Contract No. W-7405-eng-48

DIFFUSION OF IRON AND NICKEL IN  
MAGNESIUM OXIDE SINGLE CRYSTALS

Stuart L. Blank and Joseph A. Pask

May 1968

DIFFUSION OF IRON AND NICKEL IN  
MAGNESIUM OXIDE SINGLE CRYSTALS

Stuart L. Blank and Joseph A. Pask

Inorganic Materials Research Division, Lawrence Radiation Laboratory,  
and Department of Mineral Technology, College of Engineering,  
University of California, Berkeley, California

May 1968

ABSTRACT

Diffusion kinetics and mechanisms were studied in the MgO phase of the Fe-MgO (vacuum), NiO-MgO (vacuum and air), and Fe<sub>2</sub>O<sub>3</sub>-MgO (air) systems. In the Fe-MgO system Fe entered the MgO lattice by a redox reaction; the diffusivity and activation energy were found to be concentration dependent. In the NiO-MgO system in air the diffusivity was found to be concentration dependent and the activation energy, concentration independent; in vacuum both the diffusivity and activation energy were concentration independent. In the Fe<sub>2</sub>O<sub>3</sub>-MgO system the diffusivity and activation energy were concentration independent; because

---

At the time this work was done the writers were, respectively, research assistant and professor of ceramic engineering, Department of Mineral Technology of the College of Engineering, and Inorganic Materials Research Division of Lawrence Radiation Laboratory, University of California, Berkeley.

This paper is based in part on theses submitted by Stuart L. Blank in partial fulfillment of the requirements for a Master of Science degree in Engineering Science (January 1964) and for a Doctor of Philosophy degree in Engineering Science (June 1967), Department of Mineral Technology College of Engineering, University of California, Berkeley.

Presented in part at the Sixty-ninth Annual Meeting, The American Ceramic Society, New York City, May 1, 1967 (Basic Science Division, No. 2-B-67); and in part at the Eighteenth Pacific Coast Regional Meeting, Los Angeles, California, October 29, 1965.

of the 3 phase 2 moving boundary nature of the diffusion problem, the Appel modification of the Boltzmann-Matano solution was used.

Impurities in the MgO were responsible for sufficient chemically created vacancies to place the diffusion results in the extrinsic region. Formation of trivalent ions, and consequently chemically created vacancies, in the Fe-MgO and NiO-MgO (air) systems resulted in the concentration dependence of the diffusivity of primarily  $\text{Fe}^{+2}$  ions. Concentration dependence of activation energy in the Fe-MgO system is associated with development of structural changes by some of the  $\text{Fe}^{+3}$  ions moving into tetrahedral sites. In the  $\text{Fe}_2\text{O}_3$ -MgO system it is presumed that the  $\text{Fe}^{+3}$  ions remain on octahedral sites at diffusion temperatures and that the observed precipitates form on cooling. Identification of  $\text{Fe}^{+2}$  and  $\text{Fe}^{+3}$  ions and their position in the lattice were determined by electron paramagnetic resonance and optical spectroscopy.

## I. INTRODUCTION

Because diffusion plays such a significant role in all high-temperature solid-state reactions involving condensed phases, a knowledge of the diffusivities and of the diffusion mechanisms in inorganic oxides is of great practical and theoretical value. This paper reports on such studies relative to Fe and Ni ions in MgO single crystals.

Many reviews have been written on the subject of diffusion in condensed phases.<sup>1-5</sup> The vacancy mechanism is the most widely accepted for diffusion in ionic solids. At temperatures above absolute zero, the lattice of an ionic crystal contains some thermally-created vacancies. Vacancies, however, may also be created chemically. In a divalent matrix such as MgO, two trivalent ions (e.g., Fe<sup>+3</sup>) introduced into the lattice would require the formation of one cation vacancy for electro-neutrality to be retained.

The self-diffusion coefficient of Mg<sup>+2</sup> in MgO was measured by Lindner and Parfitt<sup>6</sup> using Mg<sup>28</sup> as a tracer. Their results show that at 1400-1600°C  $\underline{D} = 0.249 \exp(-79.0 \text{ kcal/RT})$ . It should be noted that this high value suggests that their material was sufficiently pure to be in the intrinsic diffusivity region.

NiO, which also has the NaCl structure, has a lattice parameter (4.177Å) similar to MgO (4.213Å). It is, however, non-stoichiometric in air containing some Ni<sup>+3</sup>. Self-diffusion coefficients of Ni<sup>+2</sup> in NiO have been determined by several investigators.<sup>7-10</sup> In the temperature range from 1000-1470°C Choi<sup>8</sup> found  $\underline{D} = 1.82 \times 10^{-3} \exp(-45.6 \text{ kcal/RT})$ .

Wüstite,  $\text{Fe}_x\text{O}$ , is also a non-stoichiometric compound with the NaCl structure. The self diffusion of  $\text{Fe}^{+2}$  in  $\text{Fe}_x\text{O}$  has been studied by Himmel<sup>11</sup> who found  $\underline{D} = 0.118 \exp(-29.7 \text{ kcal/RT})$  for a composition of  $\text{Fe}_{0.907}\text{O}$  at 700-1000°C. Roth<sup>12</sup> showed by neutron scattering techniques that the defects consisted of both atom vacancies and some  $\text{Fe}^{+3}$  ions in tetrahedral sites. Koch and Cohen,<sup>13</sup> using X-ray diffraction techniques with a single crystal of  $\text{Fe}_{0.902}\text{O}$ , identified the presence of periodically spaced clusters of vacancies, each cluster of neighboring octahedral cation sites grouped about occupied tetrahedral cation sites.

Himmel<sup>11</sup> also found that the self-diffusion of Fe in magnetite of composition  $\text{Fe}_{2.993}\text{O}_4$  (inverse spinel structure) followed the relationship  $\underline{D} = 5.2 \exp(-55.0 \text{ kcal/RT})$  in the temperature range 750-1000°C.

Hematite,  $\alpha\text{Fe}_2\text{O}_3$ , has the corundum structure with the HCP oxygen ions slightly distorted. The  $\text{Fe}^{+3}$  ions occupy 2/3 of the octahedral sites. In the temperature range 950-1050°C Izvekov<sup>14</sup> found that the diffusion of Fe in  $\text{Fe}_2\text{O}_3$  in air followed the relationship  $\underline{D} = 1.3 \times 10^6 \exp(-100,200/\text{RT})$ .

Under reducing conditions  $\text{MgO}$  and  $\text{Fe}_x\text{O}$  have been reported to form a continuous series of solid solutions at high temperature. It has been found that  $\text{Mg}^{+2}$  in wüstite does not act purely as a diluent but lowers the ratio of  $\text{Fe}^{+3}/\text{Fe}^{+2}$ . Several investigations have been made on the diffusion of Fe in  $\text{MgO}$  under various oxygen partial pressures.<sup>14-21</sup> Wuensch and Vasilos<sup>20</sup> found that the variation in diffusion coefficient with temperature in air was represented by  $\underline{D} = 8.83 \times 10^{-5} \exp(-41.6 \text{ kcal/RT})$ . Rigby and Cutler<sup>18</sup> found that the mutual diffusion coefficient in the  $\text{Fe}_x\text{O}$ - $\text{MgO}$  system was concentration dependent, but that

the activation energy was constant at 47.5 kcal/mole. In our study the activation energy as well was found to be concentration dependent.

The reaction between  $\text{Fe}_2\text{O}_3$  and  $\text{MgO}$  has been studied by several investigators.<sup>22-26</sup> Carter,<sup>23</sup> using pores as "inert" markers, stated that solid state reactions forming both  $\text{MgAl}_2\text{O}_4$  and  $\text{MgFe}_2\text{O}_4$  occurred by counterdiffusion of the  $\text{Mg}^{+2}$  and the trivalent cations through a relatively rigid oxygen lattice. He found that the ratio of ferrite formed on the  $\text{MgO}$  side of the initial interface to that formed on the  $\text{Fe}_2\text{O}_3$  side was 1:2.7 which was considered to be consistent with the diffusion of  $\text{Fe}^{+3}$ . The  $\text{Fe}^{+3}$ - $\text{Mg}^{+2}$  interdiffusion model predicts a ratio of 1:3. Fresh and Dooling<sup>26</sup> stated that at 1000-1300°C the rate controlling step in the reaction process was the diffusion of the oxide components through the ferrite product layer. Schaeffer and Brindley<sup>27,28</sup> and Ficalora<sup>29</sup> found that "fingers" and isolated "islands" of  $\text{MgFe}_2\text{O}_4$  developed in the crystals of  $(\text{Fe}, \text{Mg})\text{O}$  upon oxidation.

Speidel's<sup>30</sup> 1300°C isothermal section of the  $\text{MgO-FeO-Fe}_2\text{O}_3$  system shows that under atmospheric conditions  $\text{MgFe}_2\text{O}_4$  in the presence of excess  $\text{Fe}_2\text{O}_3$  will form solid solutions containing some  $\text{Fe}_3\text{O}_4$  as well as  $\text{Fe}_2\text{O}_3$ . It also shows the presence of some  $\text{Fe}^{+3}$  in  $\text{MgO}$  containing iron even at low pressures.

A complete series of solid solutions occurs between  $\text{NiO}$  and  $\text{MgO}$ . Hahn and Muan<sup>31</sup> have reported it to be ideal within experimental error for oxygen partial pressures between  $10^{-5}$  and  $10^{-10}$  atm. Wuensch and Vasilos<sup>20</sup> found that  $\text{Ni}^{+2}$  diffusion in  $\text{MgO}$  followed the relation  $\underline{D} = 1.80 \times 10^{-5} \exp(-48.3 \text{ kcal/RT})$ . Choi<sup>32</sup> found that the interdiffusivity and activation energy were concentration dependent. Our

study showed that only the pre-exponential term was concentration dependent in air and that neither was concentration dependent in vacuum.

## II. EXPERIMENTAL PROCEDURE

### Preparation of Diffusion Couples

Reagent grade NiO powder, \* dried at 150°C for 24 hours, was used for all of the MgO-polycrystalline NiO diffusion runs. Single crystals of MgO were purchased from the Norton Company. \*\* Diffusion couples were prepared by packing a cleaved single crystal of MgO in NiO powder in a 1/2" steel die and pressing at room temperature to approximately 5000 psi. The compacts were placed in alumina crucibles and transferred to a quench type furnace (MoSi<sub>2</sub> elements) which was used for all of the air atmosphere diffusion runs. Anneals were made in the temperature range 1200-1400°C for 25-200 hours.

Diffusion runs were also carried out in a high vacuum furnace. The same practice for sample preparation was used except that the alumina crucibles were loosely covered and wrapped in Ta foil in order to keep the oxygen partial pressure as low as possible. The system was flushed with He gas 3 times, and after each flush was pumped down to 10<sup>-6</sup> torr. The diffusion runs were made at 10<sup>-6</sup> torr. Temperatures ranged from 1200-1400°C for times from 25-150 hours.

---

\* Chemical analysis (Baker Analyzed Reagent Grade - Lot 7498): N 0.005%, Cl 0.005, SO<sub>4</sub> 0.010, Pb 0.010, Cu 0.005, Co 0.02, Fe 0.005, Zn 0.10, and alkalis and earths as SO<sub>4</sub> 0.01.

\*\* Spectroscopic analysis: Fe 0.01%, Mn 0.0015, Al 0.005, Cu 0.0015, Ca 0.01, and Cr 0.001.

A single crystal MgO vs single crystal NiO diffusion run was also made. Single crystals of NiO were purchased from Marabeni-Iida Co., Japan,\* and cleaved into samples approximately 0.5 x 0.5 x 0.5 cm. Cleaved (100) faces of both NiO and MgO single crystals were placed in contact in a die with MgO powder surrounding the two crystals, and pressed. The crystals were offset from one another in order to establish an identification of the initial interface between them. The MgO powder surrounding the two crystals allowed measurement of the single crystal vs polycrystal diffusion zone as well as the interdiffusion between the two single crystals. The diffusion specimens were removed from the furnaces, cut with a diamond saw, mounted in resin, and polished.

The Fe-MgO diffusion couples were prepared by burying a cleaved single crystal of MgO in iron powder in a recrystallized alumina crucible which was previously heated with iron powder in vacuum to 1500°C. The set-up was covered, wrapped in tantalum foil and heated in vacuum, as described before, for the diffusion runs. Runs were made at 1150, 1250, and 1350°C for given lengths of time.

---

\* Spectroscopic analysis: Mg 0.01%, Al <0.003, Si <0.005, Ca 0.007, Ti <0.003, Cr <0.002, Mn <0.002, Fe 0.008, Co <0.01, Cu <0.0008, Sr <0.003, Sn <0.005, Ba <0.001, and W <0.2.

Reagent grade ferric oxide\* was used for all polycrystalline Fe<sub>2</sub>O<sub>3</sub>-MgO diffusion runs in air. Cleaved samples of MgO were packed in the powder (after drying at 150°C for 24 hours) and pressed in a 3/4" die at approximately 5000 psi. A single crystal Fe<sub>2</sub>O<sub>3</sub>\*\* vs single crystal MgO imbedded in powdered Fe<sub>2</sub>O<sub>3</sub> diffusion run was also made at a temperature of 1330°C for 163 hours.

Diffusion specimens were normally air-cooled or cooled with the furnace rather than quenched into water in order to prevent shattering of the MgO single crystals. Several specimens, however, were quenched into cold water from 1350 and 1500°C for the purpose of obtaining specimens for EPR and optical absorption studies. All of the diffusion specimens required polishing, and in some cases carbon coating, for subsequent examinations. Polishing was accomplished by lapping with successively finer abrasives, from 600 grit SiC through 0.1µ Al<sub>2</sub>O<sub>3</sub>. The polished samples were coated with carbon by vapor deposition to render their surfaces electrically conductive.

#### Experimental Analysis

An Applied Research Laboratories electron microprobe analyzer was used to determine the diffusion profiles. The K $\alpha$  X-ray emission line was monitored for all the cations in the system. The specimen current was 0.03µa. Each spectrometer output was fed to a pulse height analyzer and then to a scaler. The data output from the electron microprobe was

---

\* Chemical analysis (Baker Analyzed Reagent - Lot 2611): Insoluble in HCl 0.104%, PO<sub>4</sub> 0.02, SO<sub>4</sub> 0.003, Cu 0.03, Mn 0.003, and Zn 0.003.

\*\* Specimen from Rio Marina, Island of Elba, Italy.

automatically typed for each reading. It was then punched on computer cards. These were fed to a CDC 6600 computer in order to apply the various correction factors necessary to convert counts to concentrations.

Specimens were prepared for the EPR studies in the same manner as for the diffusion studies. Portions of the  $\text{Fe}_2\text{O}_3\text{-MgO}$  specimens were either cleaved off or ground down in order to obtain varying concentrations of iron ions. Samples were also obtained from the diffusion zone of specimens analyzed by the microprobe in both the Fe-MgO and  $\text{Fe}_2\text{O}_3\text{-MgO}$  systems. MgO single crystals were also examined. The EPR data was obtained using a microwave spectrometer equipped with a 9 GHz klystron, a reflection cavity, and a crystal detection unit. The spectrometer was calibrated by observing the sample signals along with two standards: (a) A standard of  $5 \times 10^{+14}$  spins of  $\text{Cr}^{+3}$  in MgO ( $g = 1.987$ ), and (b) Diphenyl-picryl hydrazyl (D.P.P.H.) with a  $g$  value of 2.0037.

Optical absorption patterns were obtained on a number of the diffusion specimens from a wavelength of 250  $\mu$  to 10 $\mu$ . Two spectrometers were used: A Beckman IR-4 for the region 1-10 $\mu$ , and a Cary 14 in the 250  $\mu$ -1 region. Patterns were taken using the double beam mode thereby balancing out any peaks which may be due to gases, such as  $\text{H}_2\text{O}$ ,  $\text{CO}_2$ , etc., in the paths.

#### Mathematical Analysis

The concentration vs distance profiles for the Fe-MgO and NiO-MgO diffusion couples were analyzed by the Boltzmann-Matano<sup>1,4,33</sup> approach to determine the diffusivity variation with concentration. Graphical

solution of

$$\int_0^{C_0} xdc = 0 \quad (1)$$

defined the plane at which  $x = 0$  which is referred to as the Matano interface and corresponds to the original interface. With this value,  $D_{c=c'}$  was calculated using a computerized graphical integration and differentiation of  $c(x)$  using Eq. (2). The derivation of this equation is reported in the literature.<sup>1</sup>

$$D_{c=c'} = -\frac{1}{2t} \left( \frac{dx}{dc} \right)_{c=c'} \int_0^{c'} xdc \quad (2)$$

In the  $Fe_2O_3$ - $MgO$  system, because of the appearance of the magnesio-ferrite phase, the solution of the diffusion equation becomes a three phase-two moving boundary problem with discontinuities in the diffusion profiles as illustrated schematically in Fig. 1b for the isothermal cut shown in Fig. 1a. The Boltzmann-Matano approach is not applicable. Appel<sup>34</sup> has provided a mathematical solution which surmounts this difficulty. The resulting counterpart of Eq. (1) to determine the  $x=0$  plane, which can be referred to as the Matano-Appel interface, becomes

$$\int_0^{C_{I,II}} xdc + \int_{C_{II,I}}^{C_{II,III}} xdc - (C_{II,I} - C_{I,II}) x = 0 \quad (3)$$

where  $\chi$  is the distance the boundary has moved and  $C_{II,III}$  represents  $Fe_2O_3$  containing no  $MgO$ . For values of  $C < C_{I,II}$  the diffusivities are therefore obtained by straightforward integration of Eq. (2). For values of  $C > C_{II,I}$ , however, the diffusivities are obtained by integration of the following equation

$$D_{c=c'} = -\frac{1}{2t} \left( \frac{dx}{dc} \right)_{c=c'} \left[ \int_0^{C_{I,II}} xdc + \int_{C_{II,I}}^{c'} xdc - (C_{II,I} - C_{I,II}) \chi \right] \quad (4)$$

This approach was applied to one of the diffusion profiles. The other profiles were analyzed by a solution developed by Dorn and Blank<sup>35</sup> which is an extension of Crank's solution<sup>1</sup> for a two phase moving boundary case. In this solution the assumptions were made that the diffusivity is not a function of concentration and that the boundary did not move, i.e., the original interface is located at the boundary  $\bar{x}_{I,II}$ . These assumptions are reasonable in this particular case because the growth of the new phase was not excessive; calculations by the two independent methods gave results which differed by less than a factor of two for the same specimen. The solution is then

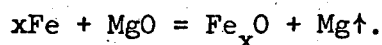
$$\frac{C_I}{C_{I,II}} = \left[ 1 - \operatorname{erf} \left( \frac{x}{2\sqrt{D_I t}} \right) \right] \quad (5)$$

from which  $D_I$  (Fe in  $MgO$ ) was calculated. This value is therefore for some average composition within the diffusion zone.

### III. RESULTS

#### Fe-MgO System

In a vacuum and in the temperature range 1100-1350°C Fe entered MgO and Mg was removed by the reaction:



A typical diffusion profile of Fe is shown in Fig. 2; no precipitates were observed. The relationship between  $\ln D$  and a/o Fe at 1150, 1250, and 1350°C, shown in Fig. 3, is linear from about 1 to 2 a/o Fe to the Fe concentration at the interface, which was constant for all times at a given temperature; the diffusivity thus shows an exponential increase with Fe concentration. Because of the source of Fe there was no moving boundary on diffusion, and the actual and Matano interfaces are thus identical. The plot of  $\ln D$  vs  $1/T$  for several concentrations of Fe is shown in Fig. 4. It can be seen from the listed values that both  $D_0$  and  $\Delta H^*$  increase with an increase of total Fe. The indicated trend in  $\Delta H^*$  was opposite to that expected. Since  $\Delta H^*$  is 30 kcal/mole in  $\text{Fe}_x\text{O}$  and 79 kcal/mole in MgO, the  $\Delta H^*$  would be expected to decrease with Fe concentration rather than increase. This behavior suggested the occurrence of structural changes in the lattice. Investigations were then made of the NiO-MgO and  $\text{Fe}_2\text{O}_3$ -MgO systems.

#### NiO-MgO Systems

Figure 5 shows a typical diffusion profile of Ni in the NiO-MgO system obtained using single crystals in air at 1370°C for 335 hours. The Matano interface, at 290 $\mu$ , which corresponds to the initial interface and represents the equal area point, lies on the high Ni side of the 25 a/o concentration point and thus indicates that a net mass flow of excess

$Mg^{+2}$ , and an equivalent amount of  $O^{=}$  ions, has occurred in this system. The result is a moving boundary. In the MgO single crystal-NiO powder couples the powders were sufficiently densified to obtain the entire diffusion profiles. The Matano interface in all cases was determined graphically, and the diffusivities were determined by the Boltzmann-Matano solution. The relationship between  $\ln D$  and a/o Ni is shown and listed in Fig. 6. The  $D_0$  term varies by a factor of about 3-4 from 2-25 a/o Ni at a given temperature in contrast to a factor of about 100 for the same concentration range in the Fe-MgO system. Figure 7 shows the  $\ln D$  vs  $1/T$  plot and lists the values for  $D_0$  and  $\Delta H^*$ . It can be seen that  $\Delta H^*$  is not a function of composition, in contrast to the Fe-MgO system.

Diffusion studies of NiO-MgO in vacuum indicated that within experimental error the interdiffusivity at a given temperature was concentration independent. The measured diffusivities were  $2.05 \times 10^{-12}$  cm<sup>2</sup>/sec at 1211°C,  $5.5 \times 10^{-12}$  at 1310°C, and  $1.09 \times 10^{-11}$  at 1400°C. The activation energy plot for these values is shown as line A in Fig. 7.

#### Fe<sub>2</sub>O<sub>3</sub>-MgO System

Figure 8 shows a typical computer-drawn diffusion profile of Fe in the Fe<sub>2</sub>O<sub>3</sub>-MgO couple heated in air at 1460°C for 42 hrs. The irregularities in the profile in MgO starting at approximately 1 a/o Fe represent ferrite precipitates formed on cooling. These increased in size as the Fe content increased. Since the limit of detection in the electron microprobe under the conditions used for analysis is estimated to be about 1 $\mu$ , the smallest detectable precipitates at about 1 a/o Fe

are probably of this order of size. At about 890 $\mu$  the concentration increases discontinuously to the atomic fraction of Fe in the ferrite; the value of about 0.32 instead of the 0.29 expected on the basis of MgFe<sub>2</sub>O<sub>4</sub> indicates the presence of some Fe<sup>+2</sup>. None of the profiles in this system indicated an excess of Mg beyond the stoichiometric amount in MgFe<sub>2</sub>O<sub>4</sub>. The peak in the profile at about 1000 $\mu$  represents a Fe<sub>2</sub>O<sub>3</sub> precipitate in the ferrite phase. Optical examination of diffusion specimens showed that the precipitates within the diffusion zone in MgO were coherent, and those in the ferrite zone, incoherent.

Diffusivities were calculated for an average composition within the diffusion zone for a number of temperatures ranging from 1020 to 1460°C according to Eq. (5). The relationship  $D = 8.83 \times 10^{-9} \exp(-74.6 \text{ kcal/RT})$  was then determined from the Arrhenius plot shown in Fig. 9. This analysis did not provide a determination of any concentration dependence if it existed.

Figure 10 shows a complete Fe profile in a couple heated at 1300°C for 43 hours. The curve represents a smooth average plot with the precipitates not shown. The Matano-Appel interface calculated according to Eq. (3) is shown at 543 $\mu$ .<sup>\*</sup> The diffusivity in MgO and ferrite was calculated by use of Eqs. (2) and (4). This analysis indicated that the diffusivity in the MgO phase was  $1.24 \times 10^{-9} \text{ cm}^2/\text{sec}$  and was concentration independent; in the ferrite phase, the diffusivity was concentration dependent with an average value of  $5.58 \times 10^{-8} \text{ cm}^2/\text{sec}$ . The diffusivity obtained in the MgO phase using the Dorn-Blank solution with the assumption

---

\* Calculation performed by M. Appel in this laboratory.

of a concentration independent diffusivity was  $6.5 \times 10^{-10}$  cm<sup>2</sup>/sec which compares favorably with the more accurate treatment. It would thus be expected that the  $\Delta H^*$  would likewise be concentration independent in the MgO phase and concentration dependent in the ferrite phase.

A single crystal MgO(001) vs single crystal Fe<sub>2</sub>O<sub>3</sub>(0001) diffusion profile made at 1330°C for 162.5 hrs showed similar features. In this case X-ray diffraction analysis using the Laue back reflection technique showed that the reaction zone of ferrite was a single crystal with its (100) face coincident with the (100) face of the MgO.

In some of the diffusion profiles Fe<sub>2</sub>O<sub>3</sub> precipitates within the ferrite zone were observed to be in direct contact with the MgO single crystal zone. Since no Mg was noted in the Fe<sub>2</sub>O<sub>3</sub> precipitates, they must not have been present during annealing and thus must have formed on cooling. A large solubility of Fe<sub>2</sub>O<sub>3</sub> in MgFe<sub>2</sub>O<sub>4</sub> at the annealing temperatures is therefore indicated. The diffusion profiles between the ferrite reaction layer and the Fe<sub>2</sub>O<sub>3</sub> were also essentially discontinuous, being less than the effective beam diameter (3μ) which indicates essentially no solubility of MgO or MgFe<sub>2</sub>O<sub>4</sub> in Fe<sub>2</sub>O<sub>3</sub>.

#### Electron Paramagnetic Resonance Studies

Figure 11 shows the EPR pattern at -160°C of the Norton single crystal MgO as received with an addition of DPPH (diphenyl-picryl hydrazyl) as a standard ( $g = 2.0037$ ). The sextet of peaks is due to octahedrally coordinated Mn<sup>+2</sup> (spectroscopic analysis shows 0.0015% Mn). Each peak is the central line of a group of 5 lines representing the  $1/2 \rightarrow -1/2$  transition, and all should be of equal intensity. The  $g$ -value, at the center of the sextet, is reported as being at approximately

$g = 2.0014$ .<sup>36</sup> The figure shows that the 4th  $1/2 \rightarrow -1/2$   $Mn^{+2}$  transition is significantly more intense than the other 5 with a  $g = 1.98$ . The pattern also shows a peak located at  $g = 1.993$ .

A standard sample of polycrystalline MgO with  $5 \times 10^{14}$  spins of  $Cr^{+3}$  ( $g = 1.98$ ) showed a  $Cr^{+3}$  peak directly in line with the 4th  $Mn^{+2}$  peak. The anomalous intensity of this peak was thus considered to be due to the chromium impurity in the original MgO material (spectroscopic analysis shows 0.001%  $Cr_2O_3$ ). Further studies showed that the peak located at  $g = 1.993$  was due to  $Fe^{+3}$  in octahedral coordination. The introduction of small quantities of  $Fe^{+3}$  into these MgO crystals by diffusion in air caused the intensity of this peak to increase and the  $g$  value to shift to higher values. Lack of magnetism in specimens with less than 0.2 a/o Fe also indicated that the  $Fe^{+3}$  ions were on octahedral sites. Heating at  $10^{-6}$  torr and  $1200^\circ C$  for 48 hrs caused the  $Fe^{+3}$  to disappear; the peak, however, was still present after heating at  $1400^\circ C$  for 1 hr and 35 min suggesting that the reduction was kinetic in nature and dependent on diffusion.

Specimens from the diffusion zone of a  $Fe_2O_3$ -MgO couple containing 0.20 a/o total iron (chemical analysis) showed similar behavior to the single crystals on heating in air and at low pressures, but with the  $g$  value for  $Fe^{+3}$  in the former case being at  $g = 2.003$ . Figure 12 shows the spectrum obtained from a section of crystal containing the entire iron profile inside the MgO. The important features are the relatively sharp transition at  $g = 2.56$  and the very broad absorption starting at approximately 1000 gauss. The figure also shows the spectrum after reduction at  $1300^\circ C$  for 10 hours ( $10^{-6}$  torr). The transition at  $g = 2.56$

has disappeared but the broad absorption band still persists but has shifted to the  $g = 2.44$  region. Both specimens were ferrimagnetic, indicating that some of the tetrahedral sites in the crystal were occupied by  $\text{Fe}^{+3}$  ions and that these were not as easily reduced as  $\text{Fe}^{+3}$  in octahedral sites. The Curie point value was approximately 330-400°C which corresponded to ferrite. The Curie point for iron metal is 770°C.

From the overall EPR results the following assignments were made. The peak at  $g = 2.0037$  which broadens and shifts to  $g = 2.56$  is assigned to  $\text{Fe}^{+3}$  coordinated in a distorted octahedral site which shifts in  $g$  value because with increasing Fe concentrations it comes closer to the vicinity of ferrimagnetic centers. The field as seen by such an  $\text{Fe}^{+3}$  will be considerably different from that seen by an  $\text{Fe}^{+3}$  in a strictly paramagnetic environment. The ferrimagnetic centers tend to concentrate the external magnetic field, and the  $\text{Fe}^{+3}$  ions would therefore see a higher local field than that measured by the gauss meter. The broad peaks in Fig. 12 are thus assigned to the ferrimagnetic resonance peak of relatively large particles of ferrite.

EPR spectra were obtained on sections from the diffusion zone in the Fe-MgO system annealed at 1200°C in vacuum. These showed the presence of a small amount of octahedral  $\text{Fe}^{+3}$  and a broad ferrimagnetic resonance peak. The latter indicated that some of the  $\text{Fe}^{+3}$  ions were occupying tetrahedral sites.

#### Optical Studies

Optical absorption studies were also made in attempting to determine the species present in the diffusion zones. Figure 13 shows the absorption pattern obtained for MgO in the wavelength region of 0.300 to 2.4 $\mu$ .

The spectrum was extended to  $10\mu$  but no significant features were found above  $2.4\mu$ . The figure also shows the spectra obtained for a specimen from the diffusion zone of a Fe-MgO couple run in vacuum which contained mostly  $\text{Fe}^{+2}$  and the same sample after heating in air for 48 hours at  $1200^\circ\text{C}$ . The appearance of a large broad peak can be seen centered about the  $0.9\text{--}1.0\mu$  region which deteriorated into a broad absorption zone; similarly, there is a significant increase in absorption below about  $0.7\mu$  which is significantly increased on oxidation. The peak centered about the  $0.9\text{--}1\mu$  region is attributed to  $\text{Fe}^{+2}$  in octahedral coordination and the absorption occurring below the  $0.7\mu$  region is assigned to  $\text{Fe}^{+3}$  octahedrally coordinated. The general increase in absorption is probably due to the appearance of ferrimagnetic precipitates indicated in the EPR studies.

Figure 14 shows four optical spectra obtained with specimens from the  $\text{Fe}_2\text{O}_3\text{--MgO}$  diffusion couples. The lowest curve is for a specimen with 0.2 a/o Fe annealed at  $1200^\circ\text{C}$  in air. A small peak can be seen at about the  $1.0\mu$  region and the optical absorption below about  $0.7\mu$  is high. The spectrum labeled "reduced" is for the same specimen after heating at  $1200^\circ\text{C}$  for 48 hours at  $10^{-6}$  torr. The peak has broadened with a general increase in absorption, and the absorption below  $0.6\mu$  has significantly decreased. EPR studies showed that no octahedral  $\text{Fe}^{+3}$  ions are present. The dashed spectrum marked "reoxidized" is again for the same specimen after reheating in air at  $1200^\circ\text{C}$  for 24 hours. The pattern marked "quenched" is for a specimen from a  $\text{Fe}_2\text{O}_3\text{--MgO}$  couple quenched from  $1350^\circ\text{C}$ . The optical spectra show a considerable concentration of octahedral  $\text{Fe}^{+2}$  ions. The iron oxide material in contact with the MgO

crystal in the latter sample was found to be  $\text{Fe}_2\text{O}_3$  and not  $\text{Fe}_3\text{O}_4$ . These observations support the fact that the nature of the Fe at temperature was different than that indicated at room temperature after slow cooling.

#### IV. DISCUSSION

##### Effect of Impurities on Diffusion Kinetics

It is known from diffusion studies on materials with the NaCl-type structure that as the vacancy concentration increases over the equilibrium concentration of thermally-created vacancies the activation energy changes from that in the intrinsic region ( $\Delta H_m^* + 1/2 \Delta H_f^*$ ) to that in the extrinsic or impurity controlled region ( $\Delta H_m^*$ ). Introduction of  $\text{Fe}^{+3}$  as impurity ions substitutionally on lattice sites in pure MgO results in chemically-created vacancies since one empty site forms for every two  $\text{Fe}^{+3}$  ions. It would then be expected that the activation energy for primarily  $\text{Fe}^{+2}$  diffusion would start at a value of about 79 kcal/mole and reach a minimum, equivalent to  $\Delta H_m^*$ , as the concentration of chemically-created vacancies with additions of  $\text{Fe}^{+3}$  or other trivalent ions approaches and exceeds that of the thermally-created vacancies. The diffusivity,  $D_o$ , would be dependent upon the concentration of vacancies.

If, however, the trivalent ions, or  $\text{Fe}^{+3}$ , should assume interstitial or tetrahedrally-coordinated sites, the resulting effect would be a structural change since these are not normal lattice sites. The local structure would tend to that for the inverse spinel. The activation energy for diffusion of predominantly  $\text{Fe}^{+2}$  in such cases would be expected to be higher than that for the extrinsic region in MgO with

substitutions on octahedral sites.

The MgO single crystals that were available at the time of this work contained a total of 0.016 w/o of elements that could be present in a trivalent state. The lower limit of trivalent impurities, as set by Al, was 0.005 w/o. The corresponding calculated concentration of chemically-created vacancies was four orders of magnitude greater than the equilibrium concentration of thermally-created vacancies in pure MgO at 1200°C. The diffusion results on these crystals then must be in the extrinsic diffusivity region, and the activation energy values should be those for the heat of motion.

#### Fe-MgO System

Both  $\Delta H^*$  and  $D_0$  in this system are concentration dependent. The  $\Delta H^*$  values increase from about 29 kcal at 5 a/o Fe to 43 kcal at 20 a/o Fe. Literature reports indicate the appearance of some  $Fe^{+3}$  in this system and analytical studies of diffusion specimens with varying iron content suggest the appearance of some of these ions on tetrahedral or non-lattice sites in the MgO. These must form by reaction when some amount of  $Fe^{+2}$  enters the lattice. Examination of an MgO structural model indicates that the presence of a  $Fe^{+3}$  ion on a tetrahedral site would require the four adjoining, or nearest neighbor, octahedral sites to be empty in order to avoid extremely high cation-cation repulsive energies. The resulting defect can also be considered as an embryonic element of the inverse spinel structure, and thus as a potential nucleus for the formation of a  $(Mg,Fe)Fe_2O_4$  precipitate on cooling. Let us now consider the effect of such an embryonic element on diffusion.

If all of the  $\text{Fe}^{+3}$  ions formed remained on octahedral sites, a vacancy would exist in the vicinity of each two  $\text{Fe}^{+3}$  ions. The bond strength between one  $\text{Mg}^{+2}$  and its coordinating  $\text{O}^{-2}$  would be only slightly increased due to the presence of the vacancy over that in pure  $\text{MgO}$ . Under these conditions the energy of motion of a vacancy in the system would not be expected to change significantly with increase of  $\text{Fe}^{+2}$  since the energy of motion of a  $\text{Mg}^{+2}$  ion would not be significantly altered. The diffusivity of  $\text{Fe}^{+2}$ , however, should increase due to the increasing number of vacancies. If a  $\text{Fe}^{+3}$  ion moves into a tetrahedral site (for an extended period of time as compared to its jump frequency), the resulting coordinated octahedral vacancies would have a pronounced effect on the bond strength of the nearby octahedrally coordinated  $\text{Mg}^{+2}$  ions. The  $\text{Mg}^{+2}$  coordinated with any of the four  $\text{O}^{-2}$  associated with the tetrahedral site could have their bond strength greatly increased. It could then be expected that the energy for motion of the  $\text{Mg}^{+2}$  ions would be increased. Since the number of tetrahedral  $\text{Fe}^{+3}$  ions increases with total Fe, this situation could then account for the increase in activation energy with increase in the Fe concentration. The diffusivity would also increase, as before, due to the increasing  $D_0$  term. Furthermore, the  $\text{Fe}^{+3}$  ions on tetrahedral sites would be expected to have considerably slower rates of diffusion than the  $\text{Fe}^{+2}$  ions; this fact plus their formation within the lattice would then account for the shape of the Fe diffusion profile.

#### NiO-MgO System

The diffusivity in this system is concentration dependent in an air atmosphere but essentially concentration independent in vacuum, and

the  $\Delta H_m^*$  is essentially the same and concentration independent in both cases. These results indicate that the concentration of  $Ni^{+3}$  ions is small or non-existent in vacuum but of sufficient amount to result in a concentration dependence of the diffusivity by a factor of 5 in an air atmosphere. Since the  $\Delta H_m^*$  is not concentration dependent, it is expected that all of the cations ( $Mg^{+2}$ ,  $Ni^{+2}$ ,  $Ni^{+3}$ ) are substitutional and remain on octahedral sites. Hence, there is no structural change. Support is gained on the basis that no known compound exists in the NiO-MgO system.

An explanation for the higher  $\Delta H_m^*$  of 42.8 kcal/mole in comparison with a value of about 29 for diffusion in the Fe-MgO system can be suggested on the basis of the octahedral preference energies for different cations in the spinel structure whose oxygen packing is similar to the MgO structure. The energy for motion of an ion should be related in some way to its relative stability or preference for octahedral and tetrahedral sites since an ion diffusing from one octahedral site to another must pass through a tetrahedral position. If the octahedral preference energy for an ion is high, the energy necessary to move it through a tetrahedral site should also be high. In this case the octahedral preference energy<sup>37</sup> for  $Ni^{+2}$  is considerably higher than that for  $Fe^{+2}$ .

#### Fe<sub>2</sub>O<sub>3</sub>-MgO System

The presence of concentration independent  $D_o$  and  $\Delta H_m^*$  terms based on the diffusion profile in the MgO phase suggests the absence of a structural change with diffusion of  $Fe^{+3}$  into the MgO. It can then be

postulated that at the test temperature  $\text{Fe}^{+3}$  ions stay on octahedral sites and that the diffusion mechanism is some complex cooperative interdiffusion between the  $\text{Mg}^{+2}$  ions and two  $\text{Fe}^{+3}$  ions and a vacancy. This complex mechanism accounts for the higher  $\Delta H_m^*$  and also means that the accompanying vacancies are not available for subsequent trivalent diffusing species, hence the concentration independence of the diffusivity. It can be further postulated that the small number of  $\text{Fe}^{+2}$  ions that are formed, or enter the  $\text{MgO}$  phase from the ferrite, stay on octahedral sites without affecting the  $\text{Fe}^{+3}$  on octahedral sites. In the  $\text{Fe-MgO}$  system at low pressures, in contrast, the dominance of  $\text{Fe}^{+2}$  ions leads to the formation of a small amount of  $\text{Fe}^{+3}$  ions which occur primarily on tetrahedral sites leading to the development of structure. On cooling the  $\text{Fe}_2\text{O}_3\text{-MgO}$  couples, precipitates of ferrite develop within the diffusion zone by rearrangement of the cations with some of the  $\text{Fe}^{+3}$  ions moving into tetrahedral sites, with possibly the existing  $\text{Fe}^{+2}$  ions playing a key role.

Weight losses have been observed on heating  $\text{Fe}_2\text{O}_3$  and  $\text{MgO}$  in air to form ferrite.<sup>22,38</sup> These would be expected to be primarily due to  $\text{Fe}^{+2}$  formation in the ferrite phase on the basis of the reported phase relations.<sup>30</sup> Since there is essentially no solubility of  $\text{MgO}$  in  $\text{Fe}_2\text{O}_3$ , interdiffusion of  $\text{Mg}^{+2}$  into  $\text{Fe}_2\text{O}_3$  results in the formation of ferrite which requires some of the  $\text{Fe}^{+3}$  ions to move into tetrahedral sites with the adjoining octahedral sites vacant. Nearby octahedrally-coordinated  $\text{Fe}^{+3}$  ions then do not have a sufficient number of vacancy sites for local charge balance thus creating a driving force for reduction of  $\text{Fe}^{+3}$  to  $\text{Fe}^{+2}$  with the removal of oxygen atoms from the

surface. Reduction of tetrahedrally-coordinated  $\text{Fe}^{+3}$  is not as easy, as verified experimentally, since  $\text{Fe}^{+2}$  ions have a high octahedral preference energy. The concentration dependence of Fe diffusivity in the ferrite phase can thus be explained on the basis of a changing structure with change in composition.

#### V. SUMMARY AND CONCLUSIONS

The MgO single crystals used had a sufficient number of vacancies due to trivalent impurities to place the diffusion results in the extrinsic region. The activation energies determined in this study thus are those for motion,  $\Delta H_m^*$ .

The results indicate that the diffusion characteristics are sensitive to the nature of the sites occupied by the incoming cations and that certain generalizations exist:

(a) If substitutional, octahedral or lattice sites are occupied, no structural changes occur and  $\Delta H^*$  remains constant; and if the number of vacancies remains constant, then  $D_0$  also remains constant.

(b) If with the diffusing species a small amount of a species of a higher valence occurs but stays on lattice sites, then with increasing cation vacancies  $D_0$  increases and  $\Delta H^*$  remains constant.

(c) If some of the small number of higher valence cations occupy interstitial, tetrahedral, or non-lattice sites, structural changes occur and  $\Delta H^*$  changes (increases in this case); these structural changes also affect the number of cation vacancies and  $D_0$  likewise increases.

(d) If the principal diffusing species is of higher valence than the host lattice cation, the resulting vacancies are not available for subsequent cations because they must in some complex way move along

with the diffusion species in order to maintain electrovalence balance, e.g., two trivalent cations and a vacancy interdiffusing with three divalent cations. The three systems studied provide examples of all these possibilities.

The use of the electron microprobe provides an atomic concentration profile; it does not distinguish between different valences of an element. The valences of the cations and their distributions must be determined or inferred on the basis of chemical and physical information available for the system. In any case, however, a profile would be expected to be continuous at the test temperature; the precipitates existing in any profile thus must have formed on cooling by localized rearrangements and short distance movements because of the short times involved.

The NiO-MgO system had a concentration independent  $D_0$  term in vacuum and a concentration dependent  $D_0$  in air; the  $\Delta H^*$  was essentially the same for both conditions. The principal diffusing species was  $Ni^{2+}$ ; in air sufficient amounts of  $Ni^{+3}$  were formed which stayed on octahedral sites.

The Fe-MgO system in vacuum had Fe ions enter the MgO lattice by reaction and showed increasing  $D_0$  and  $\Delta H^*$  values with an increasing concentration of Fe in MgO. The principal diffusing species was  $Fe^{+2}$ . In this environment  $Fe^{+3}$  was formed by reaction and its content was dependent on the amount of  $Fe^{+2}$ . Under these conditions at least some of the  $Fe^{+3}$  appeared to occupy interstitial or tetrahedral sites which corresponded to a structural change.

The  $\text{Fe}_2\text{O}_3$ - $\text{MgO}$  system in air had an intermediate ferrite compound formed by reaction which had varying solid solutions of  $\text{Fe}_2\text{O}_3$  and  $\text{Fe}_3\text{O}_4$  depending on position relative to the reacting oxides; an excess of  $(\text{Mg}, \text{Fe})\text{O}$  was not observed in any of the couples. Analysis of the Fe diffusion profile in the  $\text{MgO}$  phase indicated a concentration independent diffusivity and consequently also a constant  $\Delta H^*$  term. The principal diffusing species was  $\text{Fe}^{+3}$  which apparently stayed on octahedral sites at the test temperature. Analysis of the Fe profile in the ferrite phase showed a concentration dependent diffusivity; presumably  $\Delta H^*$  would also be concentration dependent. The principal diffusing species was  $\text{Fe}^{+3}$  probably on octahedral sites; structural complications, however, occur because some portion of the  $\text{Fe}^{+3}$  ions must be on tetrahedral sites in the ferrite phase and because some  $\text{Fe}^{+2}$  ions form by reaction which would stay on octahedral sites and contribute to the diffusivity.

ACKNOWLEDGMENTS

Grateful acknowledgment is extended to Melvin Klein and B. Spencer for assistance in the electron paramagnetic resonance analysis, to B. Evans in the use of the electron microprobe, to Marvin Appel in the analysis of some of the diffusion profiles, and to Robert Atkin for general laboratory assistance. Thanks are also given to Gabor A. Somorjai, R. J. Myers, J. E. Dorn, R. M. Fulrath, and Bette Blank for their counsel and helpful discussions.

This work was done under the auspices of the U. S. Atomic Energy Commission.

REFERENCES

1. J. Crank, Mathematics of Diffusion (Clarendon Press, Oxford, 1956).
2. W. Jost, Diffusion in Solids, Liquids and Gases (Academic Press, New York, 1931).
3. W. D. Kingery, Atom Mobility, in Introduction to Ceramics (John Wiley and Sons, Inc., New York, 1960), p. 217.
4. R. M. Barrer, Diffusion In and Through Solids (MacMillan Co., New York, 1931).
5. P. G. Shewmon, Diffusion in Solids (McGraw-Hill, New York, 1963).
6. R. Lindner and G. D. Parfitt, Diffusion of Radioactive Magnesium in Magnesium Oxide Crystals, *J. Chem. Phys.* 26, 182 (1957).
7. M. T. Shim and W. J. Moore, Diffusion of Nickel in NiO, *J. Chem. Phys.* 26, 802 (1957).
8. J. S. Choi and W. J. Moore, Diffusion of Nickel in Single Crystals of NiO, *J. Phys. Chem.* 66, 1308 (1962).
9. S. M. Klotsman, A. N. Iimofeev and I. Sh. Trakhtenberg, *Fiz. Metal. i Metalloved* 14, 428 (1962).
10. R. Lindner and A. Akerström, Diffusion of Ni<sup>63</sup> in Nickel Oxide, *Disc. Faraday Soc.* 23, 133 (1957).
11. L. Himmel, R. F. Mehl and C. E. Birchenall, Self-Diffusion of Iron in Iron Oxides and the Wagner Theory of Oxidation, *Trans. Am. Inst. Min. Met. Eng.* 197, 827 (1953).
12. W. L. Roth, Defects in the Crystals and Magnetic Structures of Ferrous Oxides, *Acta Cryst.* 13, 140 (1960).
13. F. Koch and J. B. Cohen, The Defect Structure of Fe<sub>x</sub>O, to be published in *Acta Crystallographica*.

14. V. I. Izvekov, Diffusion of Fe in Magnetite, Inzhener, Fiz. Zhur. Akad. Nauk. Belorus S.S.R. 1, 64 (1958).
15. R. Shelley, E. B. Rigby and I. B. Cutler, Note on Diffusion of Cobalt Oxide and Ferrous Oxide in Polycrystalline MgO, J. Am. Ceram. Soc. 45, 302 (1962).
16. V. H. Tagai, S. Iwai, T. Iseki, and M. S. Tokio, Diffusion of Iron, Manganese and Chromium Oxides into Single Crystal Magnesia, Radex-Rundschau 4, 577 (1965).
17. G. R. Pulliam, Decorated Dislocations in Magnesia Crystals, J. Am. Ceram. Soc. 46, 202 (1963).
18. E. B. Rigby and I. B. Cutler, Interdiffusion Studies of  $Fe_xO$ -MgO, J. Am. Ceram. Soc. 48, 95 (1965).
19. F. Nemeč, The Kirkendall Effect in the MgO-FeO System, Acta. Phys. Austriaca 18, 205 (1964).
20. B. J. Wuensch and T. Vasilos, Diffusion of Transition Metal Ions in Single-Crystal MgO, J. Chem. Phys. 36, 2907 (1962).
21. S. L. Blank, Diffusion of Iron into Single Crystals of MgO, UCRL-11073 (1964).
22. P. Reijnen, Investigations into Solid State Reactions and Equilibria in the System MgO-FeO-Fe<sub>2</sub>O<sub>3</sub>, Fifth International Symposium on the Reactions of Solids, August (1964).
23. R. E. Carter, Mechanism of Solid-State Reaction Between Magnesium Oxide and Aluminium Oxide and Between Magnesium Oxide and Ferric Oxide, J. Am. Ceram. Soc. 44, 116 (1961).
24. Y. S. Rubinehike, M. M. Pavlyuchenko, I. A. Tsybulko, and V. G. Leitsina, Dokl. Acad. Nauk Belorussk S.S.R. 8, 654 (1964).

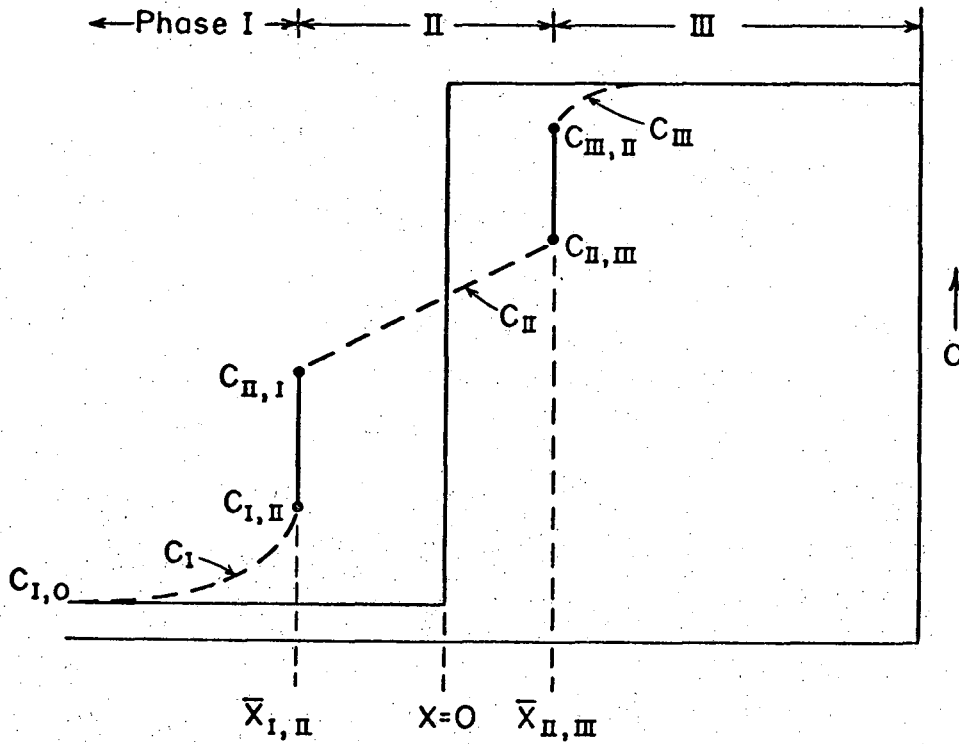
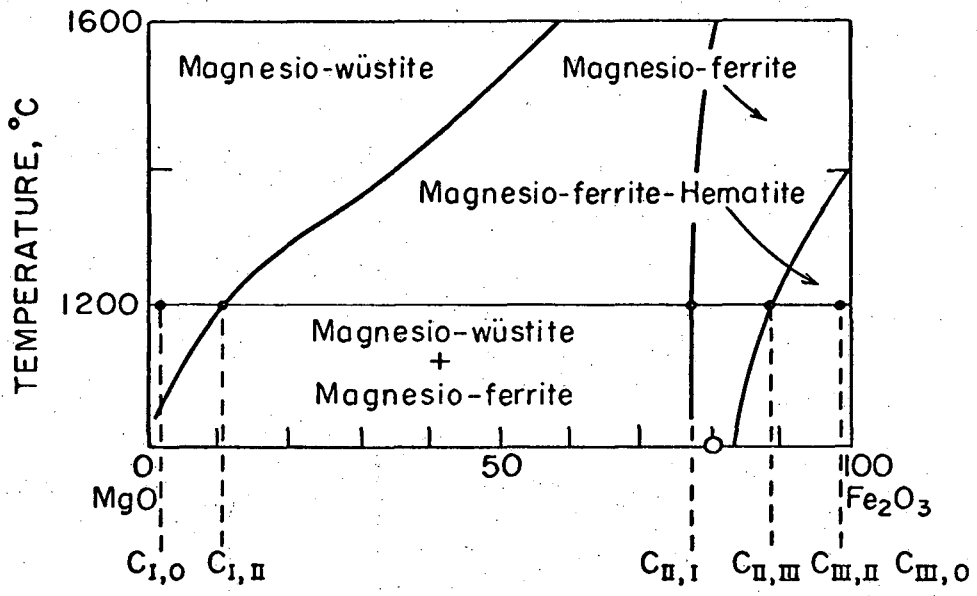
25. J. J. Comer, N. C. Tombs and J. F. Fitzgerald, Growth of Single-Crystal and Polycrystalline Thin Films of  $MgAl_2O_4$  and  $MgFe_2O_4$ , J. Am. Ceram. Soc. 49, 237 (1966).
26. D. L. Fresh and J. S. Dooling, Kinetics of the Solid-State Reaction Between Magnesium Oxide and Ferric Oxide, J. Phys. Chem. 70, 3198 (1966).
27. W. L. Schaefer and G. W. Brindley, Oxidation of Magnesiowüstite Single Crystals, J. Phys. Chem. Solids 24, 919 (1963).
28. G. W. Brindley and W. L. Schaefer, Volume Changes of Magnesiowüstite Crystals in Oxidation-Reduction Cycles, Trans. Brit. Ceram. Soc. 63, 31 (1964).
29. P. J. Ficalora, Oxidation Kinetics of Iron-Magnesium Oxide Mixed Single Crystals, Ph.D. Thesis, Materials Research Laboratory, Pennsylvania State University, 1965.
30. David H. Speidel, Phase Equilibria in the System  $MgO-FeO-Fe_2O_3$ : The  $1300^\circ C$  Isothermal Section and Extrapolations to Other Temperatures, J. Am. Ceram. Soc. 50 (5), 243-248 (1967).
31. W. E. Hahn Jr. and A. Muan, Activity Measurements in Oxide Solid Solutions: The Systems  $NiO-MgO$  and  $NiO-MnO$  in the Temperature Interval  $1100-1300^\circ C$ , J. Phys. Chem. Solids 19, 338 (1961).
32. J. S. Choi, Diffusion of Nickel in Nickel Oxide and in Magnesium Oxide, Ph.D. Thesis, Indiana University (1963).
33. L. Boltzmann, Ann. Physik. Leipzig 53, 959 (1894).
34. M. Appel, Solution for Fick's 2nd Law with Variable Diffusivity in a Multi-Phase System, UCRL-17991 (1967), to be published in Scripta Metallurgica.

35. J. Dorn and S. L. Blank, to be published.
36. W. Low, Paramagnetic Resonance in Solids (Academic Press, New York, 1960).
37. A. Miller, Distribution of Cations in Spinel, J. Appl. Phys. 30, 245 (1959).
38. L. C. F. Blackman, On the Formation of  $\text{Fe}^{+2}$  in the System  $\text{MgO}-\text{Fe}_2\text{O}_3-\text{MgFe}_2\text{O}_4$  at High Temperatures, J. Am. Ceram. Soc. 42, 143 (1959).

FIGURE CAPTIONS

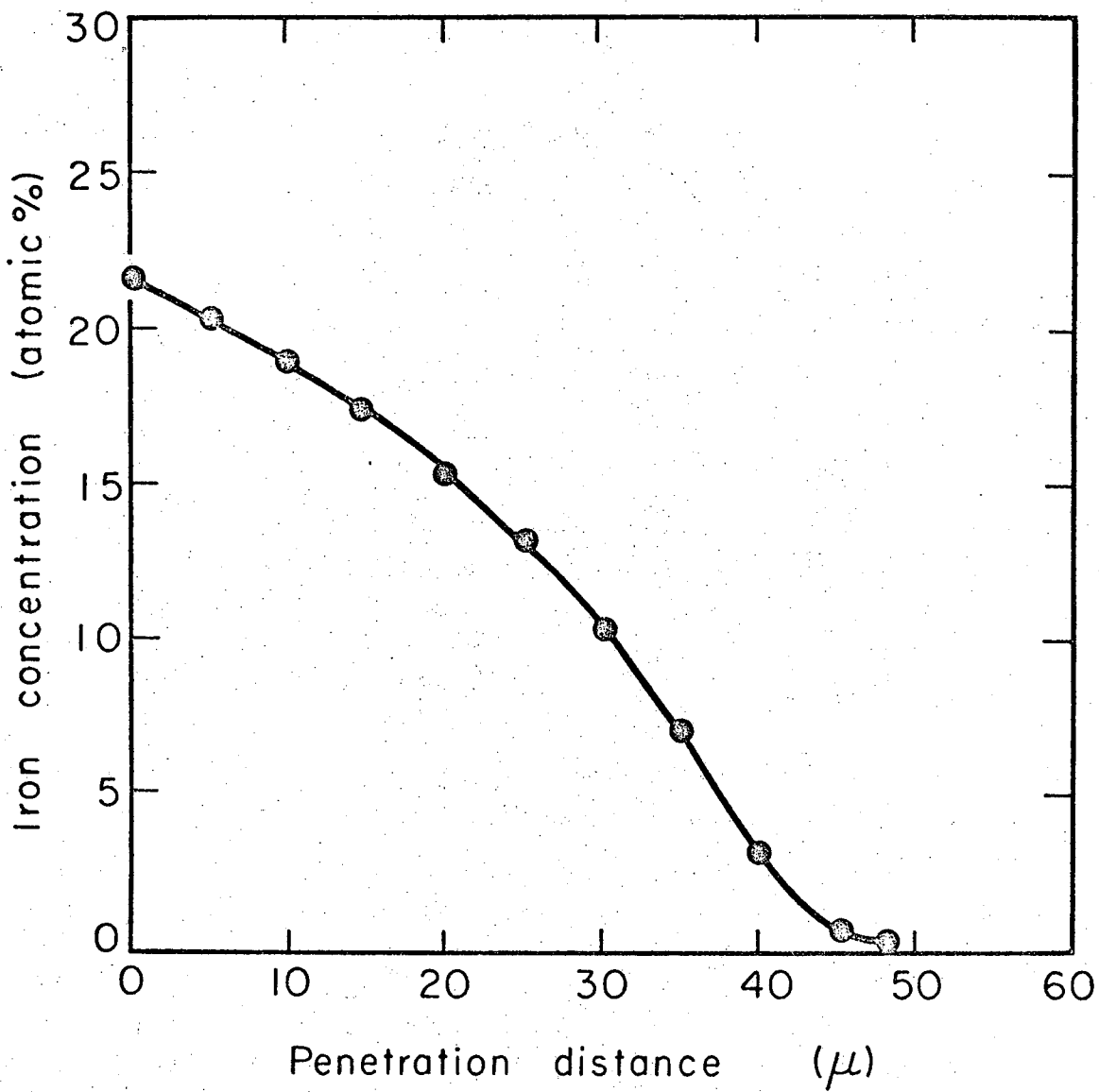
- Fig. 1. MgO-Fe<sub>2</sub>O<sub>3</sub> Phase Diagram and Schematic Diffusion Profile for Three Phase Diffusion Problem.
- Fig. 2. Typical Diffusion Profile in the Fe-MgO System in Vacuum.
- Fig. 3. Diffusivity vs Iron Concentration at 1150, 1250 and 1350°C in the Fe-MgO System in Vacuum.
- Fig. 4. Diffusivity vs Reciprocal Temperature for Several Iron Concentrations in the Fe-MgO System in Vacuum.
- Fig. 5. Diffusion Profile in the NiO-MgO System in Air at 1370°C for 335 Hours.
- Fig. 6. Diffusivity vs Nickel Concentration at Several Temperatures in the NiO-MgO System in Air.
- Fig. 7. Diffusivity vs Reciprocal Temperature for Several Nickel Concentrations in the NiO-MgO System in Air.
- Fig. 8. Diffusion Profile in the Fe<sub>2</sub>O<sub>3</sub>-MgO System in Air at 1460°C for 42 Hours.
- Fig. 9. Diffusivity vs Reciprocal Temperature for the Fe<sub>2</sub>O<sub>3</sub>-MgO System in Air.
- Fig. 10. Diffusion Profile in the Fe<sub>2</sub>O<sub>3</sub>-MgO System in Air at 1300°C for 43 Hours.
- Fig. 11. EPR Spectrum at -160°C of MgO Single Crystal with DPPH.
- Fig. 12. EPR Spectra at -150°C of Section of MgO Single Crystal Containing Entire Iron Diffusion Profile from an Fe<sub>2</sub>O<sub>3</sub>-MgO Couple, and of Same Specimen after Reduction.
- Fig. 13. Optical Spectra of MgO Single Crystal and Specimen from Fe-MgO Couple as Run in Vacuum and after Heating in Air.

Fig. 14. Optical Spectra of Specimens from  $\text{Fe}_2\text{O}_3$ -MgO Couples.



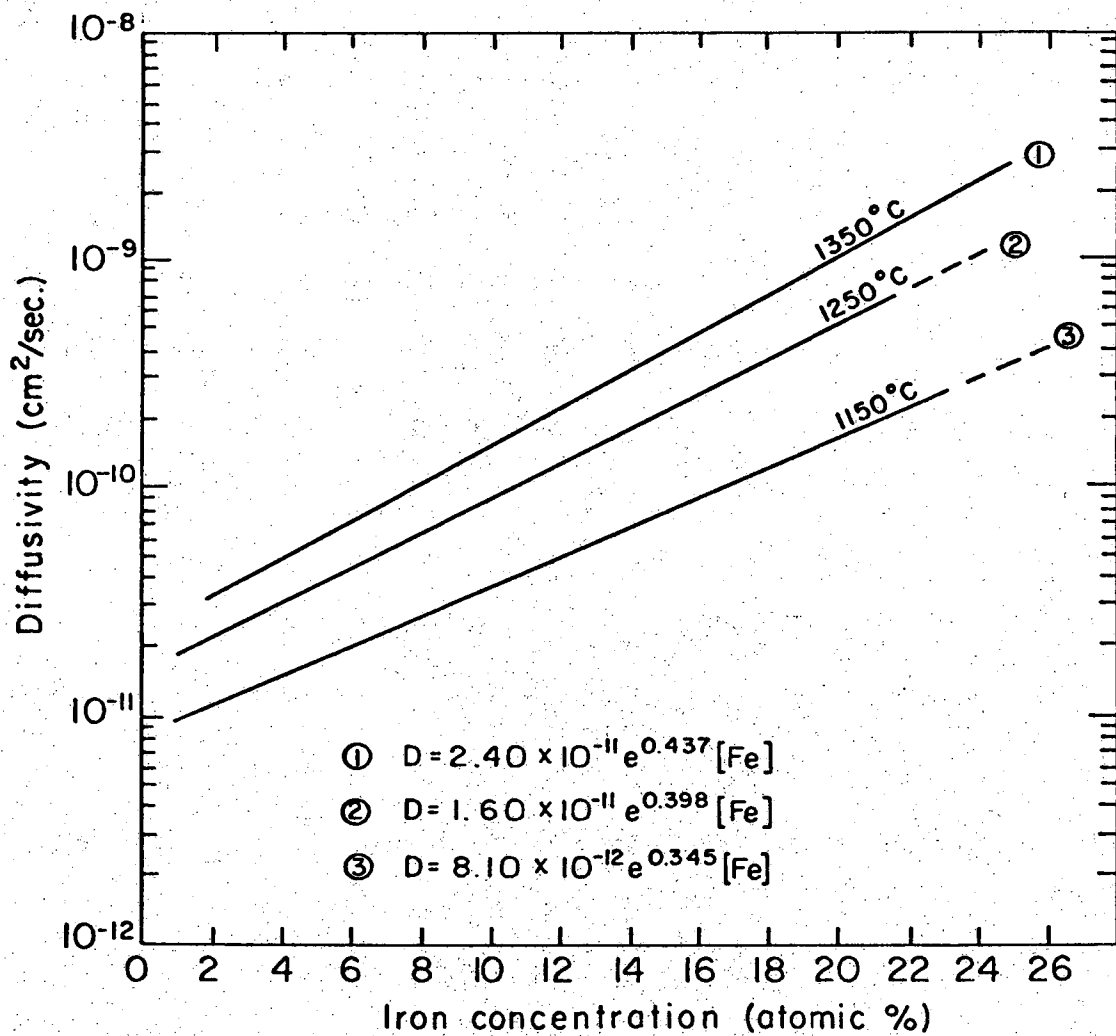
XBL 685-750

Fig. 1



MU-32845

Fig. 2



XBL 674-1034

Fig. 3

Fig. 3

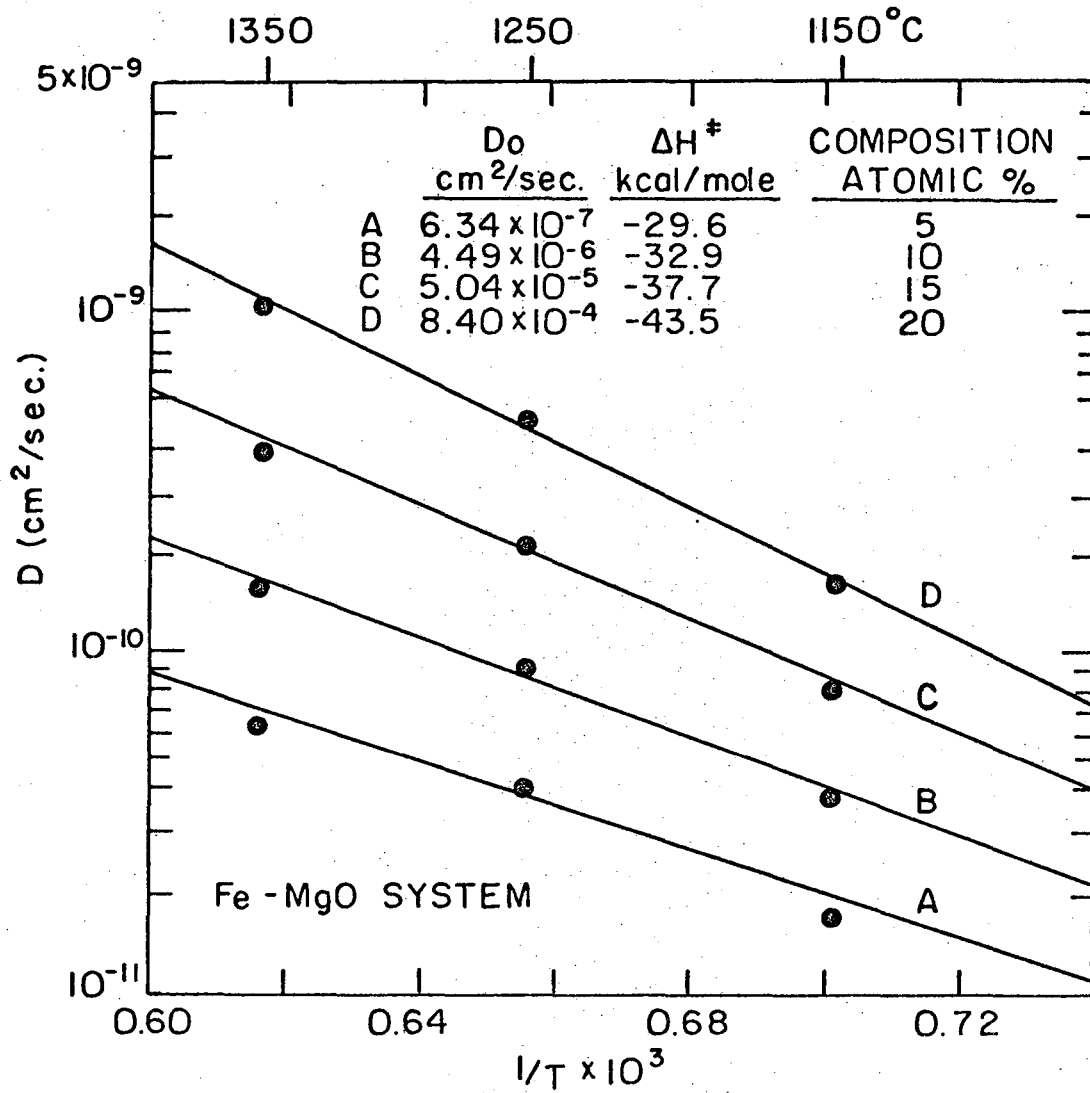
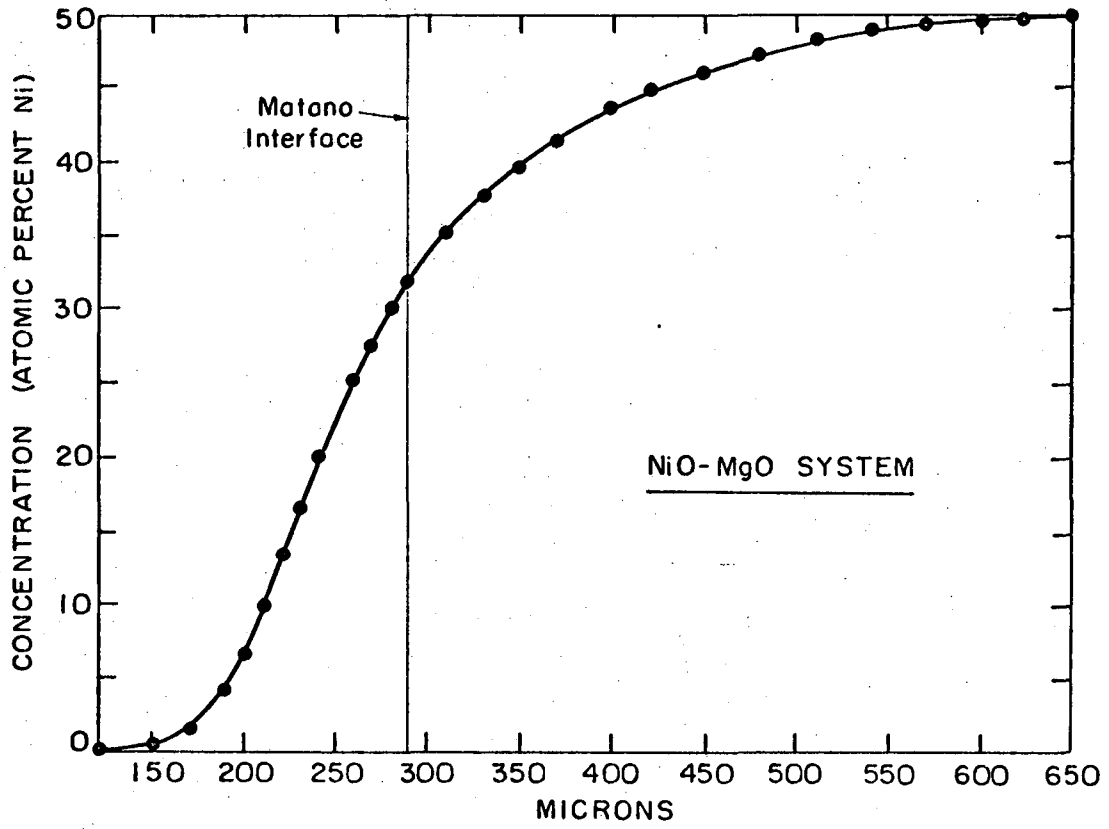


Fig. 4

XBL 674-1023



XBL 674-1024

Fig. 5

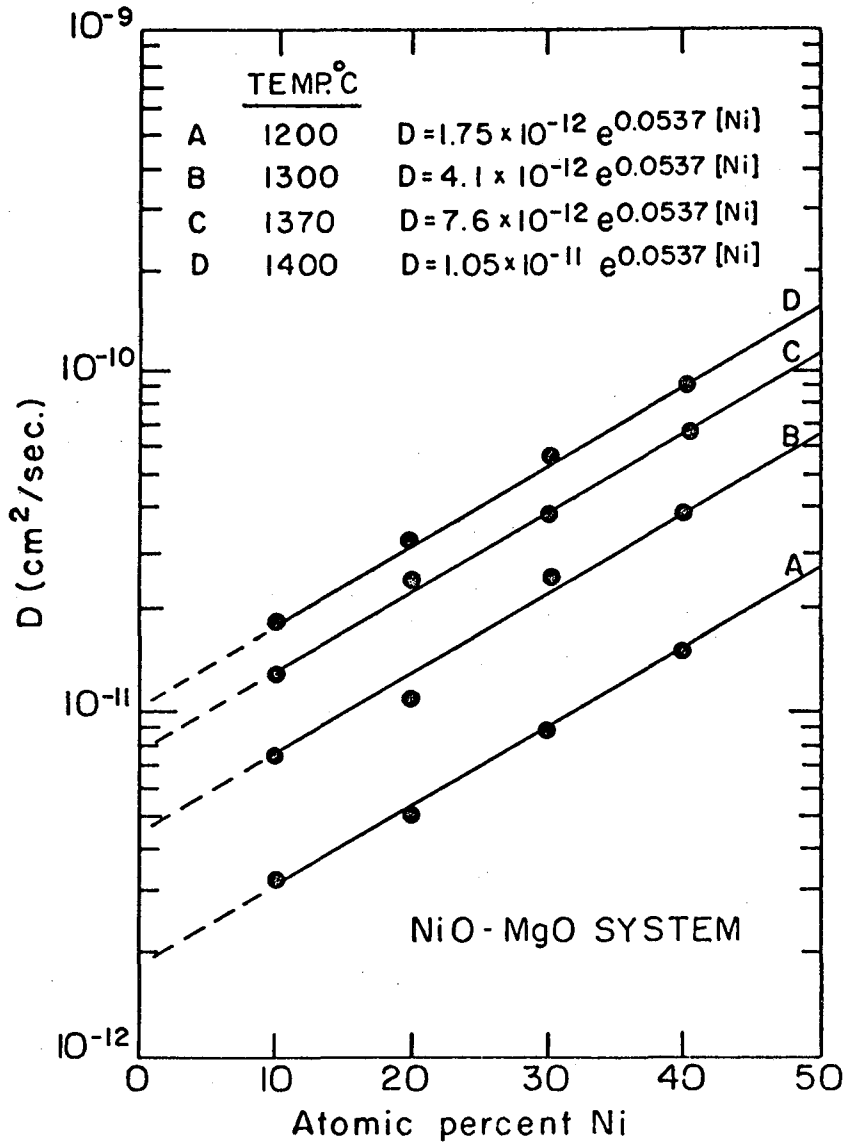


Fig. 6

XBL 674-1025

Fig. 6

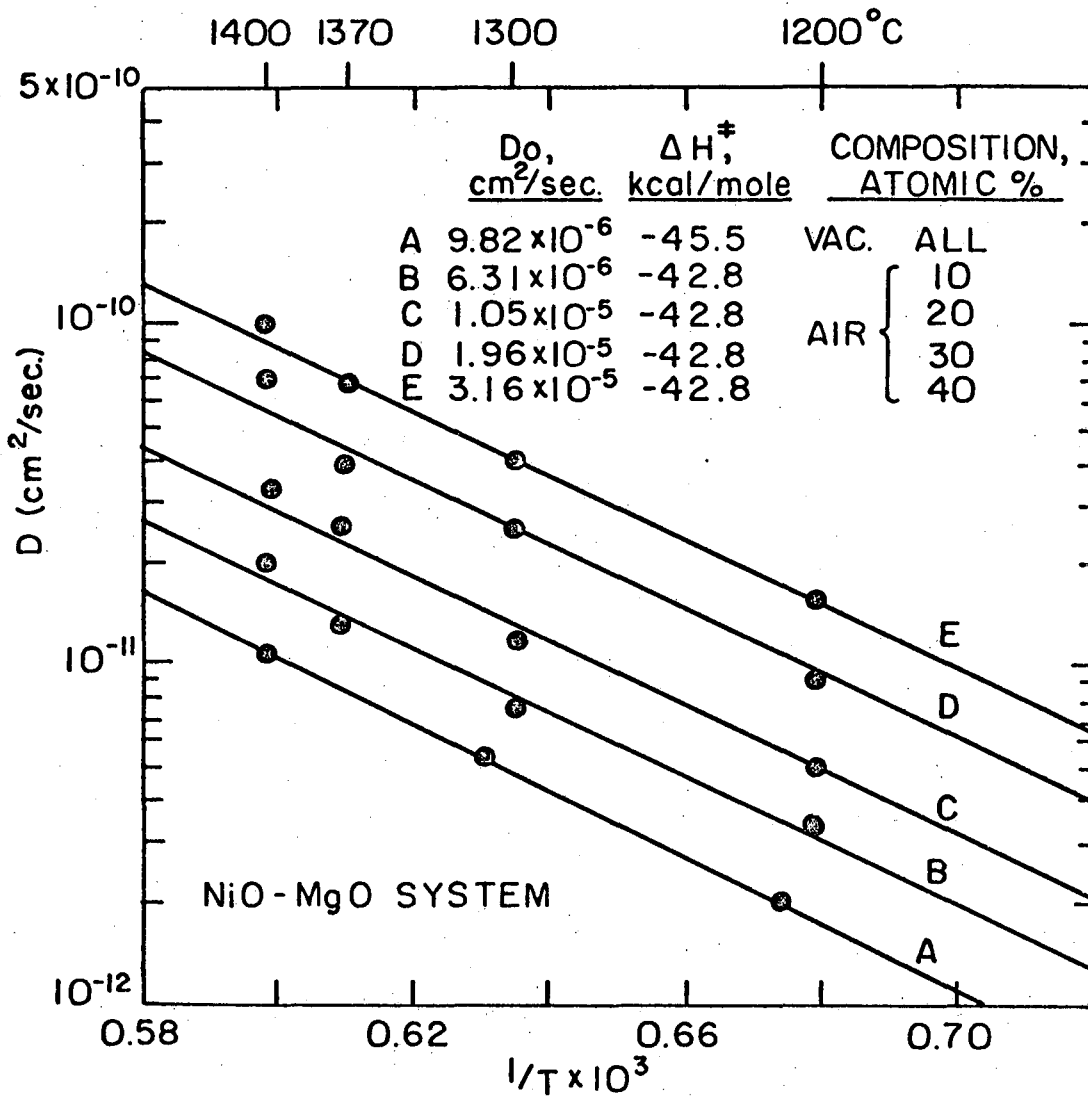


Fig. 7

XBL 674-1026

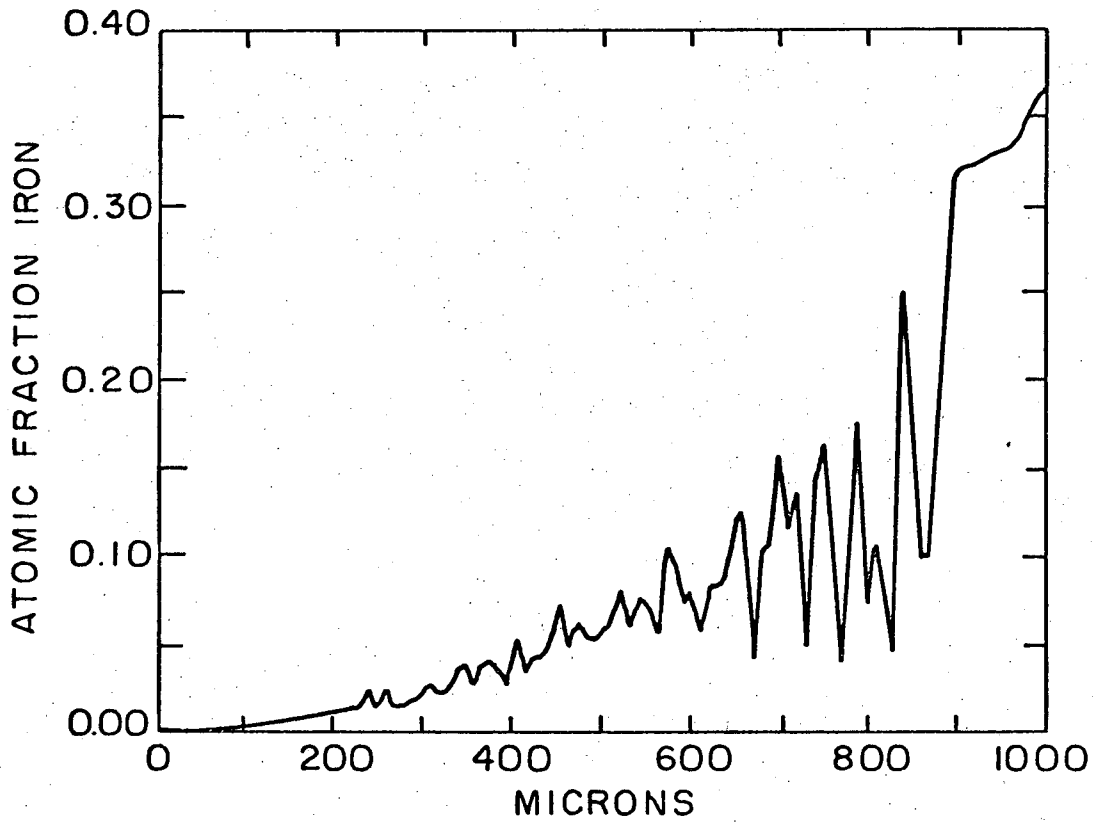


Fig. 8

XBL 674-1028

Fig. 8

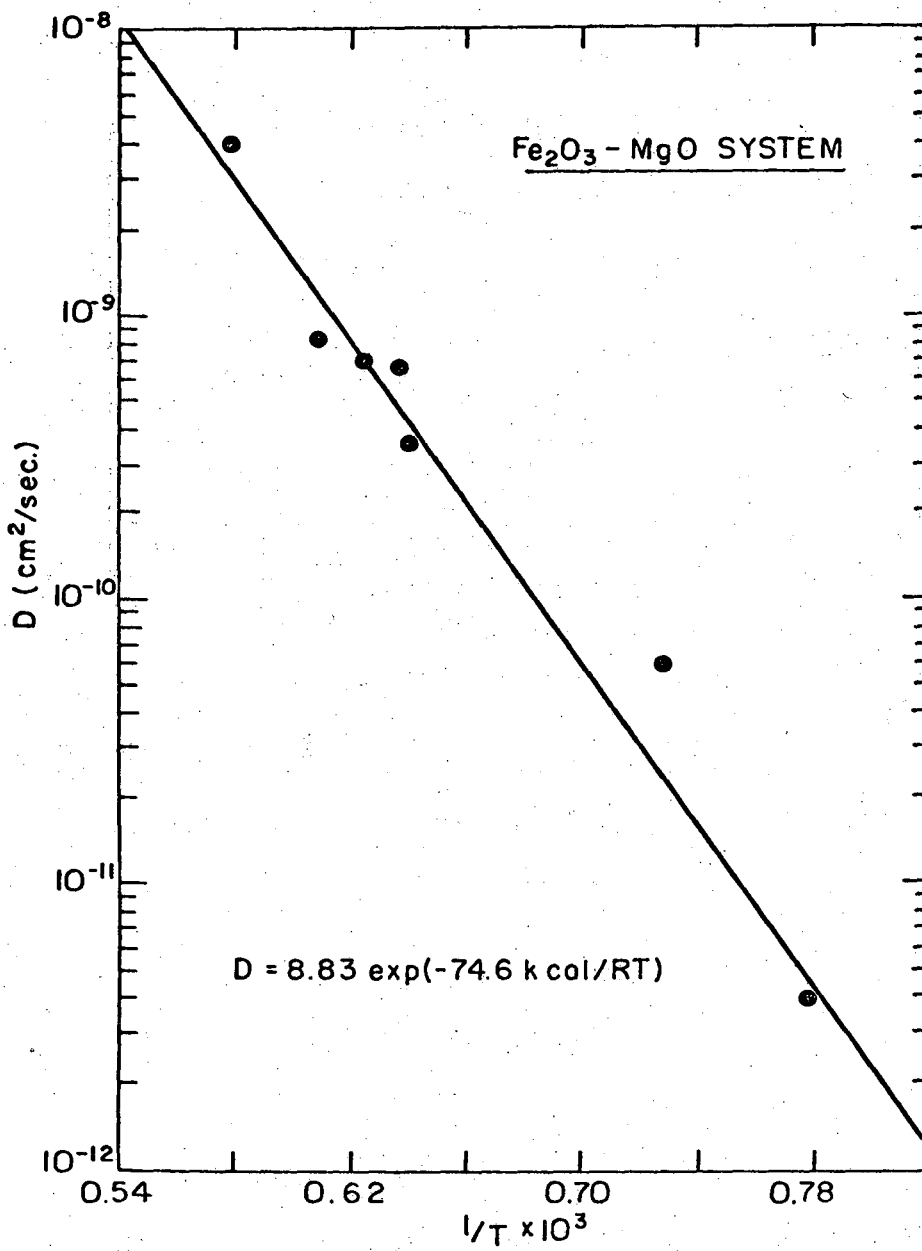
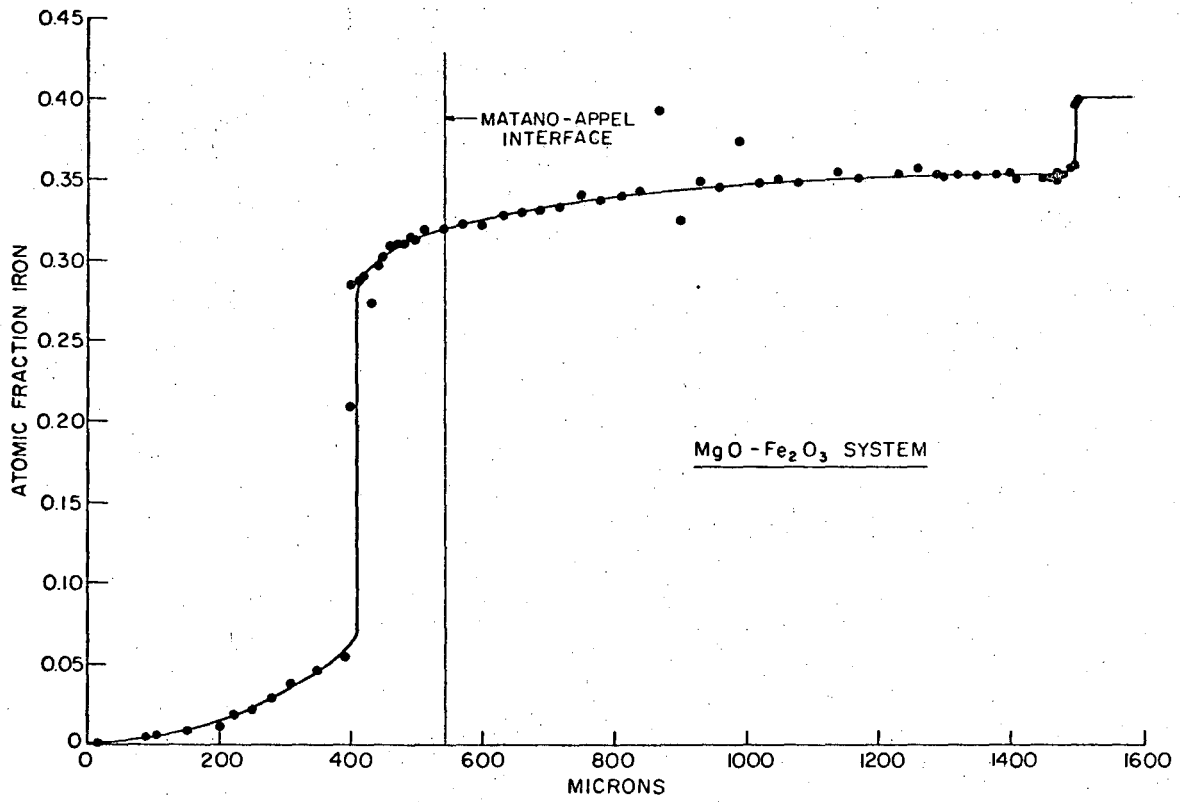


Fig. 9

XBL 674-1029

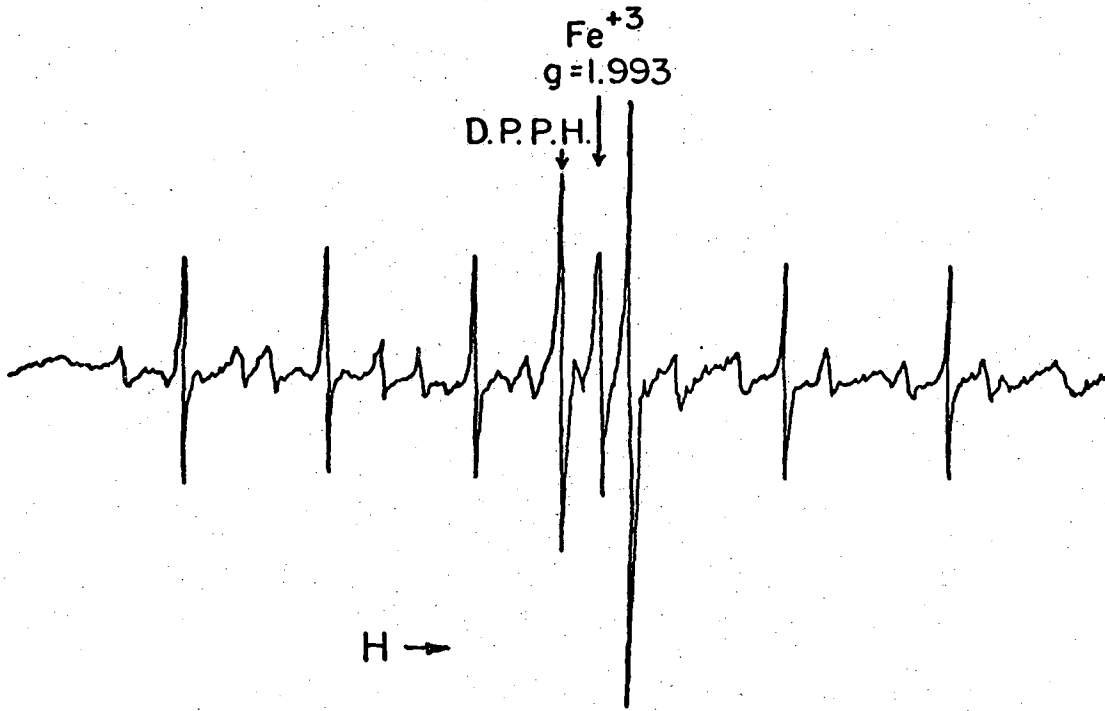
Fig. 9



XBL 695-753

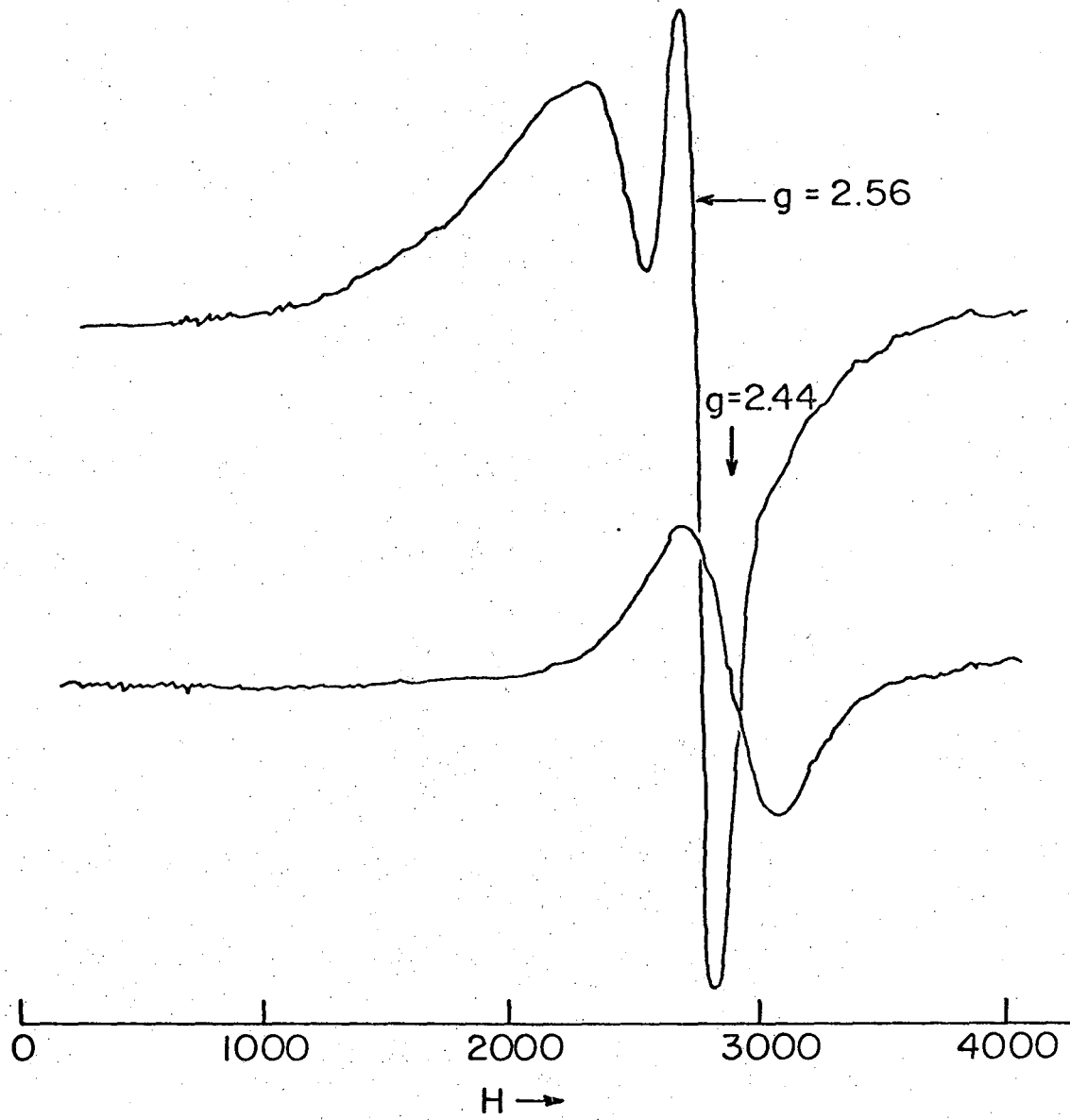
Fig. 10

Fig. 10



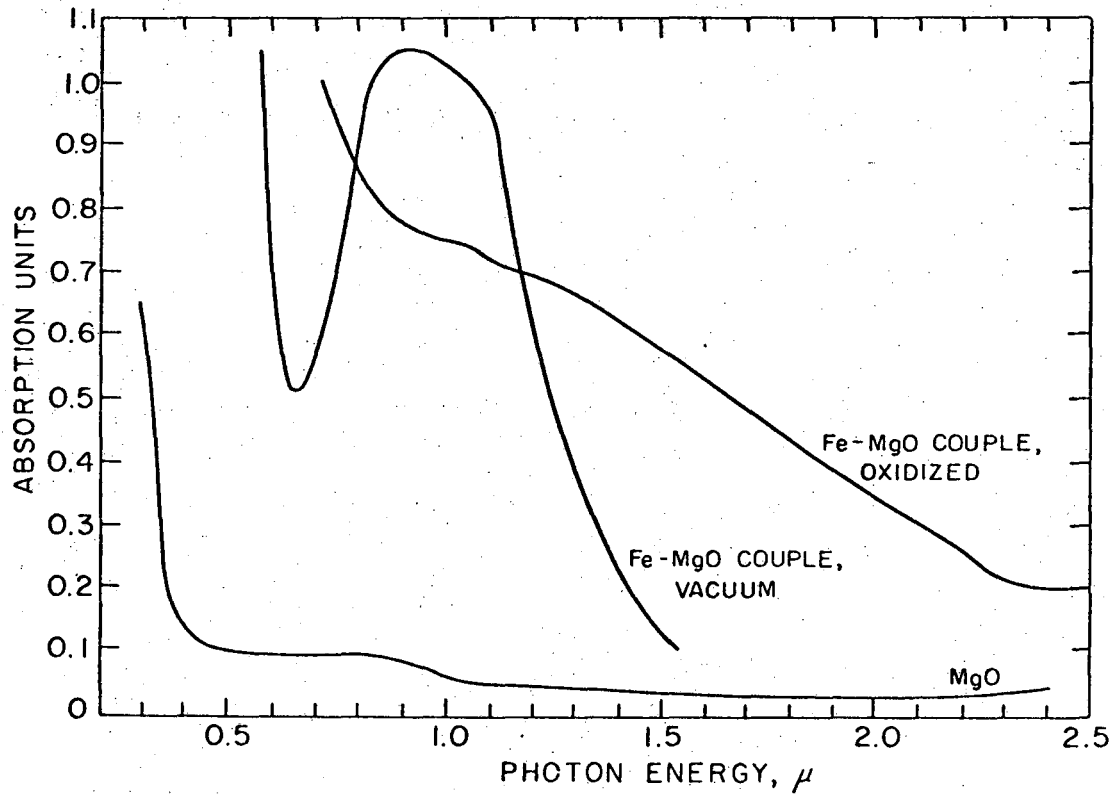
XBL 685-751

Fig. 11



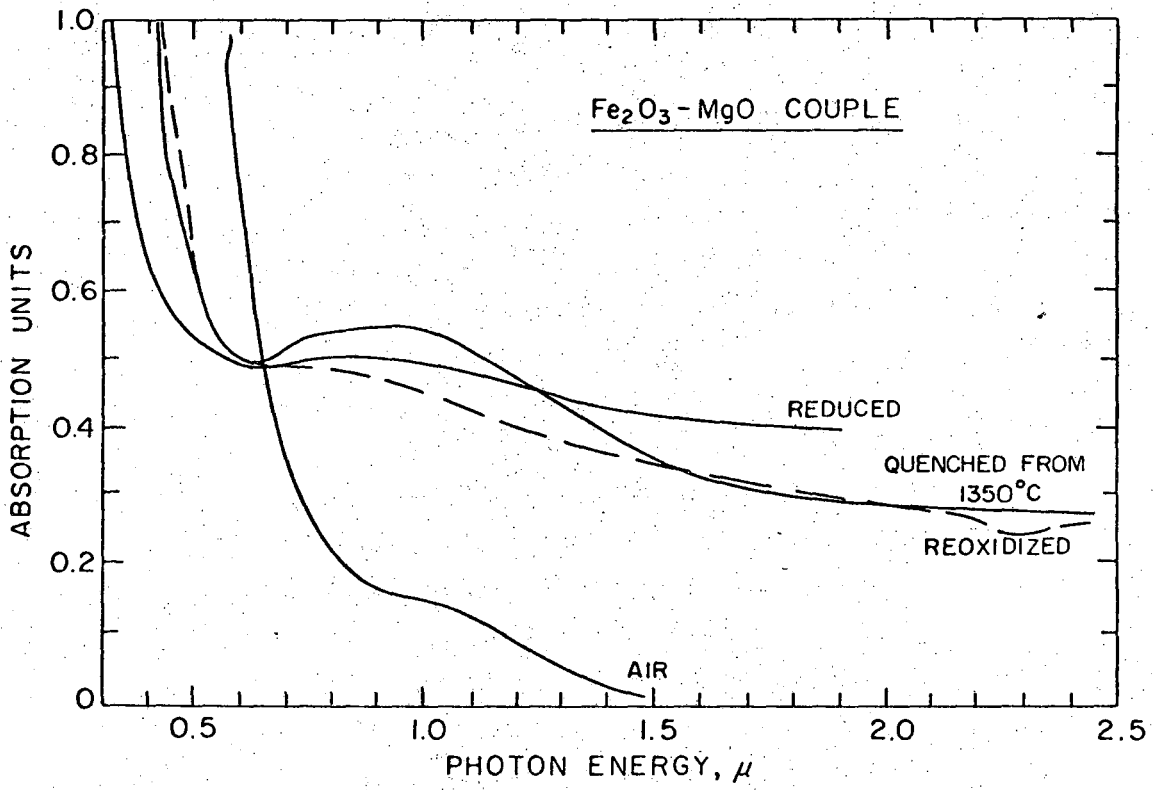
XBL 685-752

Fig. 12



XBL 674-1033

Fig. 13



XBL 674-1032

Fig. 14

Fig. 14

This report was prepared as an account of Government sponsored work. Neither the United States, nor the Commission, nor any person acting on behalf of the Commission:

- A. Makes any warranty or representation, expressed or implied, with respect to the accuracy, completeness, or usefulness of the information contained in this report, or that the use of any information, apparatus, method, or process disclosed in this report may not infringe privately owned rights; or
- B. Assumes any liabilities with respect to the use of, or for damages resulting from the use of any information, apparatus, method, or process disclosed in this report.

As used in the above, "person acting on behalf of the Commission" includes any employee or contractor of the Commission, or employee of such contractor, to the extent that such employee or contractor of the Commission, or employee of such contractor prepares, disseminates, or provides access to, any information pursuant to his employment or contract with the Commission, or his employment with such contractor.

[The text in this section is extremely faint and illegible due to low contrast and noise. It appears to be a series of lines of text, possibly a list or a set of instructions, but the specific content cannot be discerned.]

